HOVERING CRAFT & HYDROFOIL, Vol. 10, No 8, May 1971

A Geometric and Hydrodynamic Comparison Between Fully Submerged and Surface Piercing Hydrofoil Systems

by

Dr. ING. H. DE WITT

Supramar AG, Lucerne, Switzerland

ABSTRACT

By comparison of three Supramar hydrofoil types and five American test craft, important geometric parameters are found. Frictional and lifting area are plotted as co-ordinate axes for both foils and for the two main foilborne waterlines. A similar plot is represented for the area/lift ratio of both foils. The friction area of power transmission is separated from the total friction area. An estimate of induced angle is given together with the mean chord length/submergence depth ratio. The area/lift ratio yields expressions for drag/lift ratio and speed. Maximum and take-off speed are used as co-ordinate axes. Basic geometric parameters of the seakeeping capability are plotted for the design condition in smooth water and for a smaller hull clearance in a seaway.

THE following investigation refers mainly to geometric parameters that are important for the design of a hydrofoil system and which are known at an early stage in the design. In order to compare different systems, dimensionless quantities are preferred. Apart from the Russian river hydrofoils which are neglected due to their very shallow draught, the Supramar types PT 20 and PT 50 are the most successful craft for commercial applications. Since the PT 50 has nearly double the displacement and power compared with PT 20, only the PT 50 in its original shape is investigated. The largest Supramar type of hydrofoil craft is the PT 150, with a different rear foil, being

---

Notation

$a = \frac{A_d}{A_p}$	Area ratio
A_d	Developed area (half frictional surface)
ΔA_d	Referring to power transmission by inclined shaft
$A_p < A_d$	Foil plan view area (lifting surface)
b	Percentage of developed area of power transmission
c	Profile chord
d	Depth of submergence
D	Drag, $c_D = \frac{D}{q A_d}$
h	Hull clearance (distance between W.L.1 and 2)
l	Length: l_H hull waterline, l_F foil distance
L	Lift, $c_L = \frac{L}{q A_p}$
P	Continuous power of main engine(s)
$q = \frac{\zeta}{2} V^2$	Dynamic pressure
s	Foil span of submerged part
V	Speed: V_1 take-off speed (W.L.1), V_2 maximum speed (W.L.2)
W.L.	Waterline: W.L.1 touches the keel (parallel to W.L.2), W.L.2 foilborne design condition
α_i	Induced angle of attack
$\varepsilon = \frac{D}{L}$	Drag/lift ratio
$\Delta = L_f + L_r$	Maximum displacement (weight)
Index f	Front foil
Index m	Mean value, in Fig 6 measured speed
Index r	Rear foil

straight, fully submerged and air-stabilised. A third Supramar design will be considered; front foil surface piercing with W-shape and middle strut, rear foil with lateral inclined outer parts like the PT 50 but no more surface piercing. This type, on which construction is about to commence, is called PT 75 Mark III, and has both foils air-stabilised, but sufficient natural stability enables a smooth water voyage to be undertaken without the need for additional stability by air-feed.

Among the five American test craft considered here, two have surface piercing front foils, providing natural heave stability. The *Denison* has a split front foil and a small, fully submerged rear foil — a very similar arrangement to the Supramar pleasure craft ST1. The Canadian *Bras d'Or* has a canard configuration with a non-split large rear foil and a small front foil (the corresponding dihedral angles are 26° and about 40°). These two hydrofoil ships as well as *High Point* and *Plain View*, with fully submerged foils, apply Z-drives, while all Supramar types use oblique shafts. (With the exception of the German navy craft KTS 160 the construction of which has been interrupted.) Only *Tucumcari* is fitted with a water jet. The properties of a hydrofoil vessel may be sufficiently accurately described in two characteristic foilborne water lines; one for high speed in smooth water (designated W.L.2) and the other for take-off speed. The latter water line is designated W.L.1 and is defined as being parallel to the first one and touching the keel. The distance between W.L.1 and W.L.2 is called hull clearance. For the Supramar design PT 75 the water lines are not parallel and the hull clearance amounts to 0.7 m at the front foil and 0.6 m at the rear foil. The effect of pitch trim and distorted water surface on W.L.1 will be neglected.

In comparison with the available Supramar drawings, only very limited data has been published on the American hydrofoils (see list of references). This unfortunately results in less accurate figures being available for the very interesting American test craft. Any corrections offered based on more detailed drawings will be appreciated.

Comparison beween Frictional and Lifting Area of both Foils

For a certain plan view area equal to the lifting surface A_P, it must be the aim of every hydrofoil designer to get a developed area equal to half the frictional surface including struts, $A_d^* > A_P$, that is as small as possible. The limit $A_d = A_P$ can only be realised with a planing surface; not considered here. The aim of the hydrofoil designer

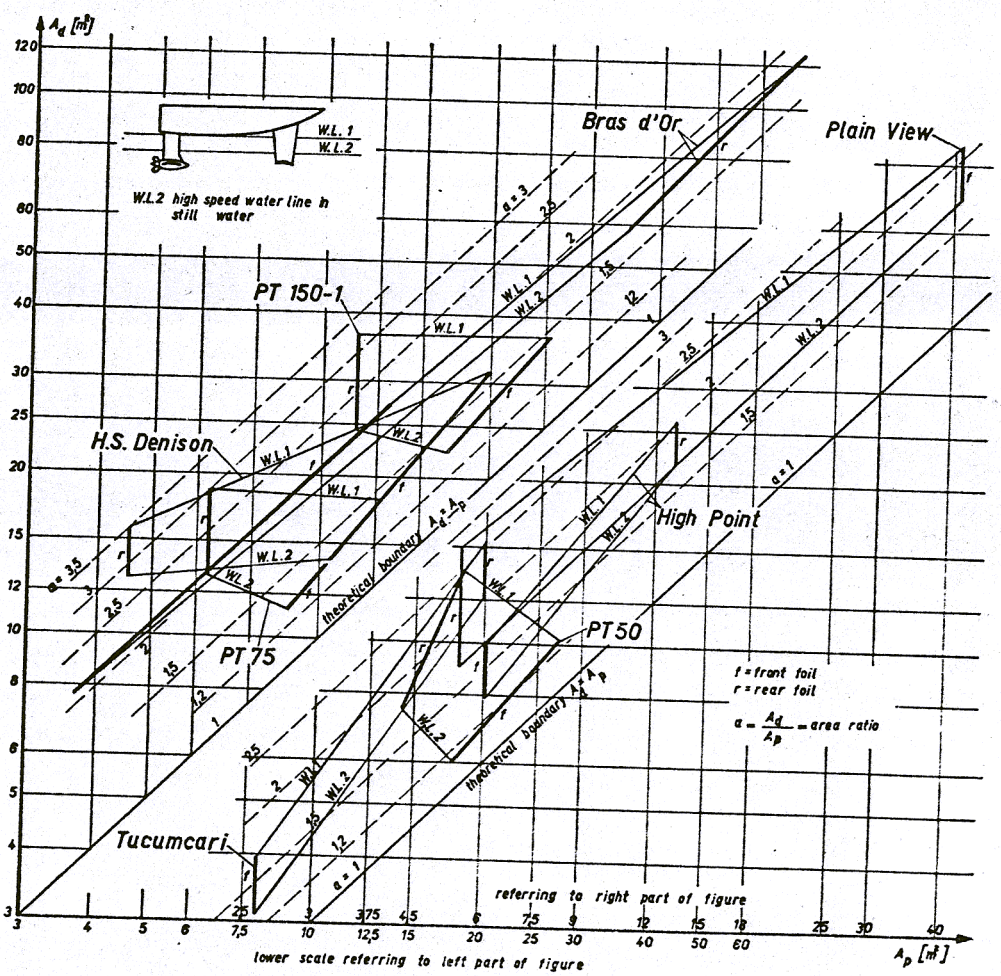

Fig. 1 Developed Area A_d and Plain View Area A_p of Both Hydrofoils of Three Supramar Typs and Five American Test Craft

to get $A_d \approx A_p$ differs from that of the aeroplane designer who takes into account a large portion of frictional area of the hull. Fortunately the hull drag of a hydrofoil ship is only a small fraction of total drag despite a relatively large cross section and unfavourable shape. Therefore, one would expect better lift drag ratios with hydrofoils compared with aeroplanes.

Fig 1 presents in a double logarithmic net on the vertical axis the developed area A_d of all submerged parts including half surfaces of nacelles, but no fences (if any), and on the horizontal axis the plan view area A_p of all surfaces producing lift by mean line camber of the profiles. Since in some parts of the diagram three or four foils would overlap, they are divided in two groups. The left/upper group refers to the lower scale and the right/lower group refers to the upper scale of the abscissa A_p. The ordinate A_d is common to all eight hydrofoil systems.

Each hydrofoil system is represented by a quadrangle of which two sides are drawn in thick lines. There the foils are represented by: f = front foil, r = rear foil. The two thinner lines refer to the water lines already mentioned. Since the lifting area A_p of fully submerged foils does not change with submergence, it appears as a vertical line in Fig 1. All other inclined straight lines would change into curves or lines having discontinuities in general, if intermediate water lines were plotted.

In spite of the simplification by interpolating intermediate water lines by straight lines, Fig 1 reveals a main geometric parameter, the area ratio

$$a = \frac{A_d}{A_p} > 1 \quad \ldots\ldots\ldots\ldots\ldots\ldots\ldots\ldots (1)$$

between frictional and lifting surfaces. This ratio is proportional to the distance from the theoretical boundary a = 1, parallel to which lines with certain parameters a = 1.2 up to a = 3.5, are dotted.

The lowest and that means best area ratio is shown by the surface piercing front foil of PT 50: a = 1.245 in W.L.1 and a = 1.134 in W.L.2. The best of the fully submerged foils represents the front foil of *Tucumcari* in W.L.2; a = 1.30 closely followed by other hydrofoils of both systems. On the other hand, *Denison* offers the worst figures on its rear foil: a = 3.48 in W.L.1 and a = 2.82 in W.L.2.

These high area ratios are due to the nacelle housing, the Z-drive and the relatively large strut. The next highest figures appear at the air-stabilised, fully submerged rear foil of PT 150-1; a = 3.19 in W.L.1 and a = 2.11 in W.L.2. In these figures the two inclined shafts with brackets and bearings are included.

The load distribution is indicated in Fig 1 by the position of the foils. With the exception of *Bras d'Or, Tucumcari* and *High Point*, the rear foils can be seen on the left of the front foils. All Supramar types so far have the load distribution: roughly 60% on front foil and 40% on the rear foil. *Plain View* and *Denison* adopt the aeroplane type with 90% of the load on the front foil while *Bras d'Or* is an example of the inverse distribution (canard type).

The long flat quadrangle of *Bras d'Or* in the neighbourhood of a = 2 looks rather strange. It extends to the left side behind the smaller PT 50 and right side over the larger *Plain View*. The length of the *Bras d'Or* main foil line is nearly the same as for the *Denison* and both are larger than for the hydrofoils of Supramar where the term reserve area is used in a similar sense. Accidentally the front foil lines of *Denison* and PT 75 fall partly together. An extreme case presents the front foil of *Bras d'Or* which extends over an area ratio between both water-lines of more than 3.5 in both directions. This unusual front foil with full ventilation of the suction side is designed to follow the wave contour and is very little affected by orbital motion.

Comparison Between Frictional and Lifting Total Area and Fraction of Power Transmission

The thick lines in Fig 2 represent the total area of both foils, which are separated in Fig 1. The scatter in Fig 2 is reduced in comparison with Fig 1 and the area ratio lies between a = 1.42 (PT 50 at W.L.2) and a = 2.18 (*Plain View* W.L.1). The fully submerged systems are characterised by vertical lines but the hybrid and surface piercing systems represent a quadrangle whose four lines are explained separately in Fig 2.

The area fraction of the submerged part of the power transmission can be taken as the vertical distance between the upper thick line and lower thin line separately for both water lines. The calculation of the area fraction involves some difficulties for all propulsion systems applied. The simplest case seems to be the inclined shaft of the Supramar types, since the shaft with brackets and bearings can be removed without impairing the foils, which are designed independently of the power transmission, apart from the suspension point of the propeller bearing at the rear foil. On the other hand, the Z-drive of the four American test craft and the water jet of *Tucumcari* are integrated into the strut design.

In order to compare the increase of the frictional surface by a Z-drive with the inclined shaft arrangement, it is necessary to analyse the integrated power transmission. This can be accomplished by comparison of this unit with

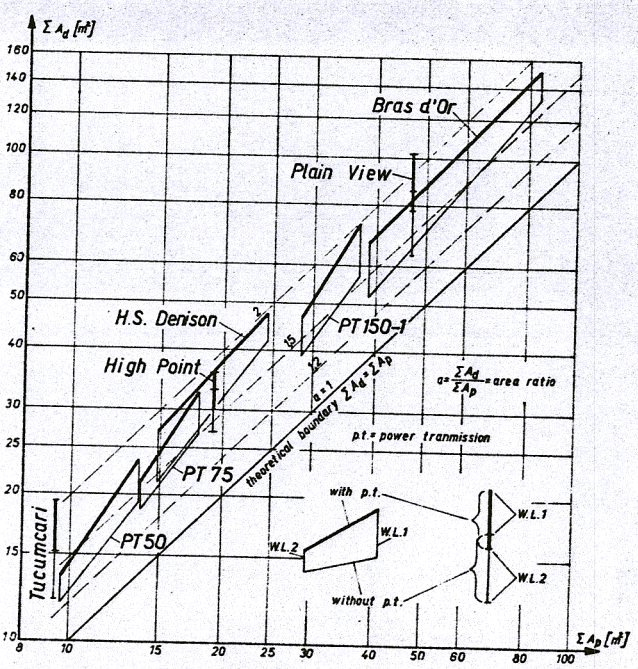

Fig.2 Total Developed Area ΣA_d With Fraction of Propulsion and Plain View Area ΣA_p of Hydrofoil Systems

* Calculating the flat plate of same chord length as a curved profile involves a small error which in general amounts to less than 1%. For 10% thickness ratio an ellipse yields 1.57% and a circular arc profile 0.67% more area than the flat plate.

the second foil unit of the vessel without power transmission. This unit shows a considerably smaller size of the strut relative to the foil, and a corresponding change of the size of the nacelles takes place. In general it is not possible to omit the nacelle completely due to the actuators for the lift control, which are housed in the nacelle.

Length and diameter of the nacelles with bevel gears have been reduced to half of their value in the compared theoretical case without bevel gears. The corresponding reduction of frictional surface yields a bit less than 3/4 from the nacelle surface. The reduction of the strut chord length by omission of the Z-drive varies between zero (*High Point*) and 30% as maximum (*Tucumcari*). These figures appear perhaps rather arbitrary but they are based on published data on the American test craft currently at the disposal of Supramar.

In relation to friction drag the surface of the nacelle is comparable with the surface of foil and strut. These surfaces depend on the similar conditions such as Reynolds number, roughness, cavitation number. On the other hand, the inclined shaft applied by Supramar cannot be compared directly with the other surfaces of the foil system, unless the ratio of their drag coefficients is known.

Let us start with an estimate of the profile drag coefficient C_{D1} which can be referred to the friction coefficient C_f of the flat plate. We assume $C_f = 0.0035$ at *fully turbulent* flow. This value corresponds to the hydraulic smooth plate at the Reynolds number $Re = 4 \times 10^6$ and to a relative sand grain roughness $c/k_s = 7 \times 10^4$ if $Re > 5 \times 10^7$. Despite many calculations of other authors who suppose partly laminar flow due to hydraulic smooth surfaces, it must be emphasised that the long term service of a hydrofoil ship like the Supramar craft unfortunately does not permit the necessary smooth surface condition for laminar flow.

With the thickness ratio of the profile t/c the drag coefficient C_{D1} yields

$$C_{D1} = 2C_f\left(1 + 2.5\frac{t}{c}\right) = \frac{D_1}{q\,A_1} \qquad \text{.....(2)}$$

$$= 2 \times 0.0035\,(1 + 0.25) = 0.009$$

where the area A_1 is identical with the developed foil area A_d or half the surface of a nacelle.

The inserted thickness ratio $t/c = 0.1$ is valid for Supramar hydrofoils up to 40 kt. The factor 2.5, which covers the super velocities mainly due to thickness, is taken from Schlichting/Truckenbrodt (Ref 10), while the last author in Ref 9 calculated values of 2.06–2.44 depending on the type of thickness distribution. Therefore, the factor 2.5 includes the additional influence of camber which Truckenbrodt (Ref 9) treated separately. The drag coefficient $C_{D1} = 0.009$ is in accordance with wind tunnel experiments of corresponding profiles at $Re = 6 \times 10^6$ and fully turbulent flow (Ref 11).

A propeller shaft with submerged length l_p, inclination α and diameter ϕ according to Hoerner (Ref 8) has a drag coefficient

$$C_{D2} = 0.01 + \tfrac{1}{2}\sin^3\alpha + \frac{\sin\alpha}{Fr^2} = \frac{D_2}{q\,A_2},\quad A_2 = l_p\phi \qquad \text{.....(3)}$$

The first term refers to friction drag, the second to pressure drag and the third one to wave drag, where the Froude-number is defined by $Fr^2 = V^2/gd_p$.* The depth of submergence of the lower shaft end can be expressed by $d_p = l_p \sin\alpha$. In what way the shaft drag depends on Reynolds number is not known. According to other authors (unpublished reports) the influence of the relatively small ratio between circumferential speed of the shaft and forward speed of the vessel is small and will be neglected.

As is to be expected, the drag coefficient of the shaft is larger than of other underwater parts; $C_{D2} > C_{D1} = 0.009$. With the ratio of both drag coefficients we define an equivalent area of the shaft:

$$\Delta A_{d2} = A_2\frac{C_{D2}}{C_{D1}} \qquad \text{.....(4)}$$

This must be added to the frictional area of brackets and bearings ΔA_{d1} which are calculated with C_{D1}. If we denote the area components of the power transmission by the inclined shaft $\Sigma\Delta A_d = \Delta A_{d1} + \Delta A_{d2}$, their percentage of the total frictional area is

$$b = \frac{\Sigma\Delta A_d}{\Sigma A_d + \Sigma\Delta A_d} \qquad \text{.....(5)}$$

Fig 2 shows that for the three Supramar types the equivalent area of the oblique shaft arrangement is increased from W.L.2 to W.L.1, absolutely and relatively. The percentage amounts to, $b = 12.6\%$–18.8% for PT 50 and $b = 17.0\%$–22.3% for PT 150, while the figures for PT 75 are only slightly above those of PT 50. The marked increase from the 60 t/80 t-range to 160 t (PT 150) seems to confirm a conclusion drawn by Faber (Ref 12) who estimates a limiting transmission power of 5,000 hp per shaft.

On the other hand, the area ratio of Z-drive components total area (nacelle and enlarged strut) decreases with increasing depth of submergence and the absolute additional area $\Sigma\Delta A_d$ increases only slightly. The lowest percentage is shown by *High Point*; $b = 10\%$–8% in the water lines W.L.2 and W.L.1, respectively. These unrealistically low figures are due to the tandem propeller arrangement which did not prove to be feasible for continuous operation. The other three craft with Z-drives are between $b = 19\%$–23% in W.L.2 and $b = 13\%$–16% in W.L.1. The corresponding figures for *Tucumcari* are 21% and 20%. The larger value in W.L.1 compared with the Z-drive results from the large strut chord length necessary for the water intake. The effective frictional area is still larger since the ribs inside the rudder are replaced by fences outside.

Summarising we can state the following general results:

(a) The inclined shaft arrangement yields in the low speed foilborne water line (W.L.1) about the same drag percentage as the Z-drive in the high speed water line (W.L.2).

(b) As can be seen in Fig 2 about 30% lower drag percentage than in case (a) is yielded by the inclined shaft arrangement in the high speed water line and the Z-drive in the low speed water line.

(c) The relative drag increase due to water jet propulsion is — independent on depth of submergence — as high as in case (a). It is true that this statement is less reliable than the former two since only *Tucumcari* has been analysed, but it confirms theoretical considerations.

Since the main foils in Fig 1 are represented including power transmission, some area ratios $a = A_d/A_p$ without power transmission in W.L.2 may be mentioned. We find the best values on *Tucumcari*, *Plain View* and *Bras d'Or*, with $a = 1.30$. The main foil of the American test craft is considered as being the larger foil carrying the higher load than the other foil of the tandem having no Z-drive or water jet. An exception is the *Denison*. On the other hand, the inclined shaft of Supramar types is always connected to the smaller rear foil. The area ratio of PT 50 in W.L.2 amounts to $a = 1.366$ without, and $a = 1.76$

* g = acceleration due to gravity.

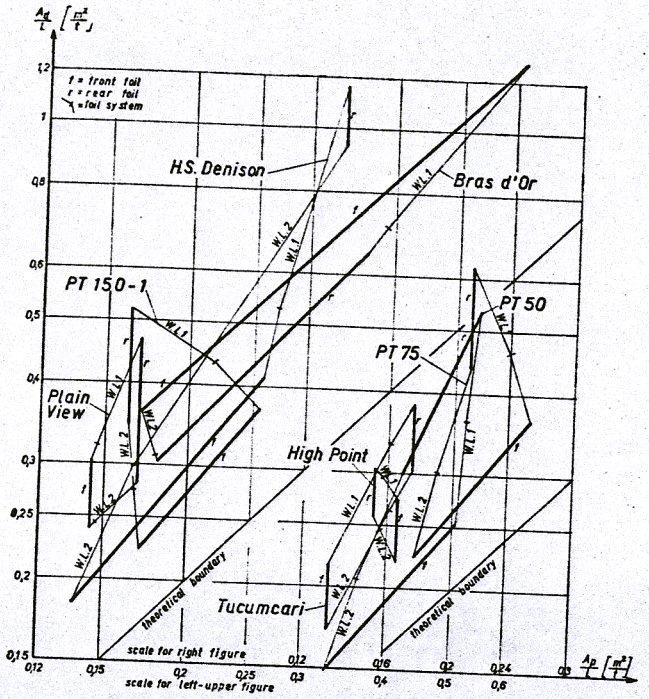

Fig. 3 Area of Both Hydrofoils as Ratio to the Generated Lift

with power transmission. In the order of increasing area ratios this foil ranges in fifth place. But in connection with the excellent front foil a = 1.134 shown in Fig 1, PT 50 is by far the best hydrofoil craft with all four corners of its quadrangle represented in Fig 2.

Area of Both Foils as Ratio to the Generated Lift

The double logarithmic net of Fig 3 corresponds with the former ones, but frictional and lifting surface are divided by the respective lift L. Thus the ordinate represents A_d/L and the abscissa A_p/L which is the inverse value of the well known loading. The points situated furthest to the left and bottom in Fig 3 represent foils which need the least area to produce the necessary lift, which favours low friction drag and foil weight.

The points belonging together, are connected again by thick lines: f = front foil, r = rear foil. The high speed water line W.L.2 is represented by thin lines at the left or lower side of the quadrangles. Only *Denison* shows an intersection of this line with the other one representing W.L.1 which touches the hull and is parallel to the high speed water line W.L.2. All thin lines have a discontinuity marked by a small stroke relating to the whole craft $\Sigma A/\Delta$. The displacement Δ must be in equilibrium with the sum of foil lift; $\Delta = L_f + L_r$.

The point situated furthest to the left belongs to the front foil of PT 50 in W.L.2. Compared with the design condition the displacement of this Supramar type was gradually increased by safety demands of the classification societies. The loading of this foil, which is similar to the front foil loading of *Tucumcari* and *Denison*, corresponds with 3/4 of the atmospheric pressure — that means at least ten times the loading of an aeroplane. The discontinuities in the lines for the eight hydrofoil systems in the high speed water line 2 are gathered around the coordinates $\Sigma A_d/\Delta = 0.26\ m^2/t$ and $\Sigma A_p/\Delta = 0.16\ m^2/t$. On the other hand, the corresponding points in the low speed, but still foil-borne, water line 1 are scattered along a straight line $\Sigma A_d/\Sigma A_p = 1.9$ analogous with the area ratio "a" in Fig 2.

An inaccuracy of the load distribution on both foils would shift the points of Fig 3 parallel to the theoretical boundary but would not affect the points of the whole system as discussed. Some qualifying points should be mentioned:

(a) The static lift of all submerged parts, especially nacelles. According to Supramar experience all hollow parts are filled with water after a continuous operation of a certain period which may not be reached with the American test craft. Hereby most of the static lift is lost.

(b) The pressure drag D_p of the inclined shaft is combined with lift $L_p = D_p\ \mathrm{ctg}\alpha$ which may be larger than the total drag of the shaft. A larger lift force is generated by the propeller due to the inclined flow.

Subtracting the dynamic lift of propeller and shaft or the static lift of nacelle and other submerged parts from the dynamic lift of the foil would shift the corresponding points in Fig 3 parallel to the theoretical boundary.

Induced Angle of Attack and Ratio Between Foil Chord and Depth of Submergence

The straight elliptical foil of large aspect ratio AR without sweep induces the negative angle of attack

$$\alpha_i = \frac{C_{Di}}{C_L} = \frac{C_L}{\pi AR} = \frac{1}{\pi}\frac{L}{qb^2}, \quad AR = \frac{s^2}{A}, \quad L = C_L q\, A, \quad q = \frac{\rho}{2} V^2$$

This well known formula yields the minimum induced angle which is increased by the vicinity of the free surface, dihedral angle and the limited Froude number of a hydrofoil. Complications are added by interference between both foils. Depending on the foil configuration, positive and negative angles of attack can be induced at the rear foil.

On account of this complexity it seems to be better for the simple geometric treatment of this study to omit the factor $1/\pi$ in the classic relationship and to use only

$$\alpha_i^* = \frac{\Delta}{q\, s^2} \qquad \text{.....(6)}$$

which nearly gives the right value for surface piercing V-foils. The maximum span of immersed foil parts is denoted by s; for example the distance between the piercing points in W.L.2 of the split front foil of the *Denison* whose rear foil is situated in the gap of the front foil. In this way the whole foil system could act as a single foil of span s. In the case of fully submerged foils the maximum beam of the main foil, it may be split or not, is inserted in the definition of the induced angle α_i^* equation (6).

The dynamic pressure q in general is based on the calculated speed according to the section on speed dealt with later. For *Denison* and *Bras d'Or* the measured maximum speed at W.L.2 is taken.

In Fig 4 α_i^* is plotted as abscissa, where the upper left points refer to W.L.2. The corresponding group of Supramar craft shows the largest induced angle of attack but the rear foil of PT 50 and PT 75 with dihedral angle at the outer foil parts wins back a considerable part of the wave energy lost by the front foil. The trough behind the surface piercing front foil contains in the transverse plane at the position of the rear foil, transverse velocity components which induce positive angles of attack. This

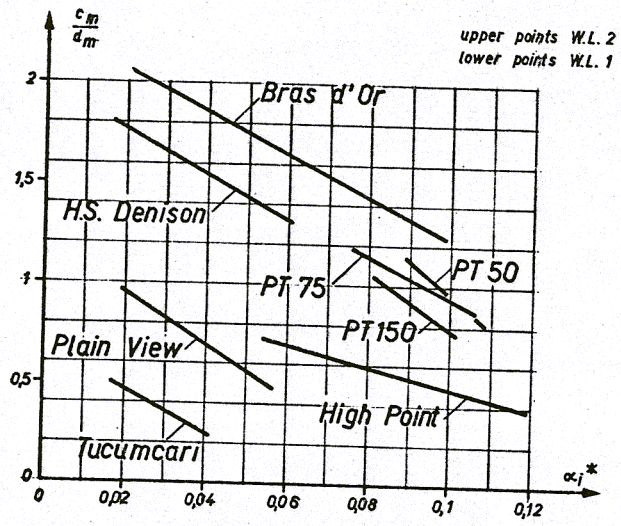

Fig. 4 Mean Values of Chord/Depth Ratio c_m/d_m and Induced Angle of Attack α_i^* of Hydrofoil Systems

phenomenon was verified by tank tests with different rear foil models behind a V-shaped front foil model.

The remarkable increase of α_i^* from W.L.2 to W.L.1 for *Bras d'Or* reflects mainly the large speed difference between V_2 and V_1 which is calculated in the section on speed. Similar relationships can be found for *Denison*. Apart from these two vessels the range of the induced angle is relatively smaller for the Supramar surface piercing hydrofoils than for the fully submerged systems, where the ratio of α_i^* between the two water lines considered is over 2.2.

Apart from *Bras d'Or*, Fig 4 shows two groups of foil systems separated by $\alpha_i^* \approx 0.06$: on the left side with split main foil and on the right side with non-split foils. The split foil systems possess in general a larger span s — needed in equation (6) — than the non-split combinations. But the theoretical low α_i^* value of the split systems can be realised only provided there is a proper position of the three foils in the plan view and a certain lift distribution along the span. The ordinate in Fig 4 represents the ratio between the mean submerged foil chord length and the mean depth of submergence based on the plan view area A_p. If ΣA_p and Σs refer to the sum of the lifting surface and corresponding beam (span) of both foils, the mean profile chord of the hydrofoil ship is $c_m = \Sigma A_p / \Sigma s$.

The mean depth of submergence has been calculated according to:

$$d_m = \frac{\Sigma(\Delta A_p d)}{\Sigma A_p}$$

where ΔA_p refers to a straight foil part and d to its mean depth (centre of area) below the water surface. The sum of both foils ΣA_p has already been used in Fig 2. The ratio of the two mean values yields

$$\frac{c_m}{d_m} = \frac{(\Sigma A_p)^2}{\Sigma s \times \Sigma(\Delta A_p d)} \quad \ldots\ldots\ldots\ldots (7)$$

Note always that $\Sigma s > s$, used in the induced angle α_i^* equation (6), where the foil tandem was treated as one foil.

The lower points of the hydrofoil ships in Fig 4 refer to W.L.1 and the higher points to the high speed W.L.2. The three fully submerged systems are situated nearest to the abscissa and *Tucumcari* reveals the smallest induced and wave making drag. Their advantage for seakeeping capability must be paid for by a worse area ratio $a = \Sigma A_d / \Sigma A_p$ according to Figs 2 and 5. The ratio c_m/d_m between the two water lines amounts to nearly two considering the three fully submerged systems in Fig 4, and varies only between 1.25 – 1.4 for the Supramar types. Note the relatively shallow submergence of *Bras d'Or* and *Denison* which will be further investigated later.

The function between c_m/d_m and "a" is represented in Fig 5. It is restricted to the low speed — but still foilborne — waterline 1 and excludes all parts of the submerged foil system necessary for power transmission, as the lower points in Fig 2. The foils are marked by letters f and r and the foil system by a small stroke where the line has a discontinuity as in Fig 3.

The Supramar foil systems PT 50, PT 75 and the front foil of PT 150 form in both waterlines a narrow group of the surface piercing configuration. Two similar groups are formed by the fully submerged foil systems *Tucumcari*, *High Point* and *Plain View* including the fully submerged rear foil of PT 150*. The centres of these four groups are marked by points designated by symbols whereby the number refers to the waterline. It may be seen that in the high speed waterline 2 the chord/depth ratio c_m/d_m of the fully submerged configuration amounts only to 2/3 of the value of the surface piercing configuration. At the same time the area ratio $a = A_d/A_p$ is increased by 5%. The respective numbers in the low speed, foilborne waterline 1, are a reduction 2.3 : 1 of c_m/d_m and an increase of "a" by 19%.

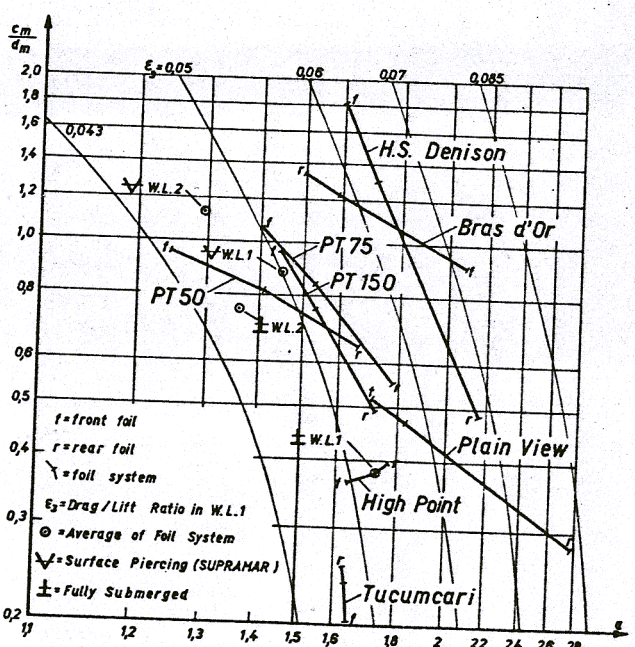

Fig. 5 Mean Value of Chord/Depth Ratio c_m/d_m and Area Ratio a of Hydrofoils Without Power Transmission in Waterline 1

* A double counting of PT 150 is avoided by application of the normal load fraction as "weight" to both foils.

Drag/Lift Ratio

It is known that the drag of a hydrofoil craft consists mainly of friction drag — a similar situation as for displacement vessels. The drag/lift ratio of the friction drag can be written as

$$\varepsilon_1 = \frac{D_1}{L} = C_{D1}\, q \frac{A_d}{L} \quad \text{.....(8)}$$

where the drag coefficient $C_{D1} = 0.009$ is taken from Ref 2 and the ratio A_d/L [m²/t] is plotted in Fig 3. Since the last ratio seems to be, as presently known, no direct function of speed or size, and C_{D1} is kept constant, the drag/lift ratio ε_1 increases proportionally to the dynamic pressure $q = \frac{\zeta}{2} V^2$.

The following assumptions are made for the high speed W.L.2.

(a) the total drag $\Sigma D = 1.61\ D_1$ or the friction drag D_1 yields 62% of the total drag,

(b) the overall efficiency is $\eta = 0.5$ — in general too low for subcavitating propellers and too high for water jet propulsion,

resulting in

$$\varepsilon_2 = 1.61\ \varepsilon_1 = C_{D_2}\, q \frac{A_d}{L}, \quad \text{.....(9)}$$

$$C_{D_2} = 1.61\ C_{D_1} = 0.0145$$

The lift can be written as $L = C_L\, q\, A_p$ and inserting this expression in (9) we get

$$\varepsilon_2 = \frac{C_{D_2}\, q\, A_d}{C_L\, q\, A_p} = 0.0145 \frac{a}{C_L}, \quad a = \frac{A_d}{A_p} \quad \text{.....(10)}$$

Taking the maximum measured speed of PT 50, V = 38.5 kt according to Fig 6 and its area/lift ratio $A_d/L = 0.207$ m²/t, which is the lowest of all hydrofoils plotted in Fig 3, we get the total drag/lift ratio $\varepsilon_2 = 0.061$ or L/D = 16.4.

Model tests with non-rotating shafts resulted in $\varepsilon = 6.7\% - 7.7\%$ depending on model weight and foil angles of attack. With the assumed efficiency $\eta = 0.5$ we get $\varepsilon_2/\eta = 0.122$. Putting this value in Fig 3 of the well known investigation of G. Gabrielli and Th. von Kármán, Ref 13, the PT 50 at V = 44.3 miles/hr appears very near to the destroyer. According to our assumptions the drag/lift ratio increases with the square of the speed and the corresponding straight line through the mentioned PT 50 point is placed to the left and above the best values of most vehicles, including helicopters, automobiles and ships.

Despite the different objects and assumptions compared with the present study of hydrofoil ships, the author obtained the same total drag/lift ratio, 6.1%, at the maximum speed of PT 50 according to Ref 14, if the single foil value 4.6% is multiplied by the factor 4/3 in order to obtain the value corresponding to the whole vessel. Since in the theoretical study of Ref 14 the Froude number has been kept constant — $\Delta \sim V^6$ — provided geometric similarity is maintained — the assumption of constant area/lift ratio made in our equations (8) and (9) is no longer valid. But the size of the vessel, rapidly increasing with speed, means larger and deeper submerged foils enabling a higher loading or smaller area/lift ratio A_d/L. This results in a drag/lift ratio only slightly increasing with speed, whereby the hydrofoil ship is placed in a better position in Fig 3, from Ref 13, namely among propeller aeroplanes.

Looking for the maximum allowable lift coefficient during *take-off* we choose the following function of the chord/depth ratio

$$C_L = 0.4 + \frac{1}{4} \exp\left(-\frac{c_m}{d_m}\right) \quad \text{.....(11)}$$

According to this formula the lift coefficient varies between $C_L = 0.420$ at the shallow submerged front foil of *Denison* (W.L.2, $c_m/d_m = 2.5$) and $C_L = 0.605$ at the deep submerged front foil of *Tucumcari* (W.L.1, $c_m/d_m = 0.2$). Model tests with Supramar surface piercing foils showed C_L values higher than 0.420 and on the other hand fully submerged foils corresponding to aeroplanes reach higher values than 0.605 though nose cavitation limits the maximum lift coefficient of a hydrofoil to less than in air. In any case the lift equation (11) leaves a certain margin for take-off in a seaway.

The increased lift coefficient during take-off yields an increase of the foil drag coefficient. Additionally, thicker strut sections with correspondingly stronger spray are immersed in W.L.1. It is therefore necessary to increase the factor 0.0145 in ε_2 equation (10) which is valid only for W.L.2. We increase the drag according to the measurements published in Ref 11 by 20% and put the assumed lift coefficient C_L equation (11) for W.L.1 in the following drag/lift ratio

$$\varepsilon_3 = \frac{0.0174\ a}{0.4 + 0.25 \exp\left(-c_m/d_m\right)}, \text{ (W.L.1)} \quad \text{.....(12)}$$

This function of the chord/depth ratio c_m/d_m and the area ratio $a = A_d/A_p$ is plotted in Fig 5 for some values between $\varepsilon_3 = 0.043$ and 0.085.

In respect of the drag/lift ratio the extreme values are reached by the front foil of PT 50 ($\varepsilon_3 = 4.5\%$ or lift/drag ratio L/D = 22) and the rear foil of *Plain View* ($\varepsilon_3 = 8.2\%$, L/D = 12). However, the extreme foil systems are represented by *Tucumcari* as the best one ($\varepsilon_3 = 4.8\%$, L/D = 21) and *Denison* as the worst one ($\varepsilon_3 = 6.3\%$, L/D = 16). The reader may remember that we are discussing the low speed waterline 1 — touching the keel parallel to the high speed waterline 2 — as a substitute for the real inclined take-off waterline.

As mentioned in the last section, the four circles in Fig 5 represent the two main hydrofoil groups; the surface piercing Supramar system and the fully submerged system applied to most American hydrofoil craft. Only the two points which belong to the W.L.1 can be related to the curves with constant drag/lift ratio. We read for the Supramar system $\varepsilon_3 = 5.0\%$ or L/D = 20 and for the other one $\varepsilon_3 = 5.24\%$ or L/D = 19. In the frame of our assumptions it can be stated — neglecting the problem of power transmission — that for take-off condition in relation to lift/drag ratio the shallowly immersed Supramar system with relatively small frictional area is equivalent to the fully submerged system with relatively large frictional area.

Speed

Based on the calculations in the last section we are looking for simple formulae to obtain the take-off speed V_1 in W.L.1 and the high speed V_2 in W.L.2.

If we insert $D = 1.61\ D_1 = 1.61\ C_{D1}\, q \Sigma A_d$ corresponding to our relationship in equation (9) in the power formula $P = V \Sigma D/\eta$, a simple relationship for the maximum continuous speed can be deducted:

$$V_2\ [\text{kt}] = 7.1 \left[\frac{P\ [\text{PS}]}{\Sigma A_d\ [\text{m}^2]}\right]^{\frac{1}{3}} \text{(W.L.2)} \quad \text{.....(13)}$$

on which the dynamic pressure q for the calculation of the induced angle α_i^* equation (6) in W.L.2 is based.

Table I: Data of vessels investigated

Hydrofoil Ship	Supramar Type				*Bras d'Or*	*Tucumcari*	*High Point*	*Plain View*
	PT 50	PT 75	PT 150	*Denison*				
Full displacement Δ [t]	66	80	170	90	215	58	122	320
Continuous foilborne power P [PS] shp	2200	3300	6880	14000	22000	3200	6200	28000
Relative load on front foil [%]	61.5	62.5	58.5	85	10	31	30	90
Foil distance l_F [m]	19.6	20.4	26.1	20.0	27.9	13.4	≈18.5	≈36.1
Ship length (hull waterline) l_H [m]	24.2	26.3	32.7	28.2	44.8	20.1	33.5	≈60.0
Hull clearance (distance W.L.1–2) h [m]	0.7	0.7/0.6	1.2	1.52	3.20	1.33	1.52	2.54
Submerged total foil beam s [m] W.L.1	8.08f	9.68f	13.80f	13.72f	20.1r	11.76r	9.60r	21.6f
Submerged total foil beam s [m] W.L.2	6.0f	7.60f	10.40f	10.28f	14.1r	11.76r	9.60r	21.6f

f = front foil, r = rear foil; W.L.1 = waterline 1 touching the keel, W.L.2 = high speed waterline

It would be reasonable to use the maximum power, but this is mostly unknown for naval craft. Therefore the published continuous power is used, as given in Table I. Changing the status of power would affect only the factor 7.1 in equation (13). The ratio between maximum and continuous power amounts for instance to 2700 PS (shp): 2200 PS (shp) = 1.23 : 1 at PT 50 (diesel engine). As shown in Fig 6, the factor 7.1 fits well to the measured maximum speed of PT 50 and PT 150. The calculated values for *Tucumcari, High Point* and *Plain View* are some knots higher than the published data. A discrepancy between calculated and measured maximum speed appears for the *Bras d'Or* craft. This may be due to an unexpectedly high maximum turbine power or a particularly smooth surface reducing the drag coefficient below our standard value 0.009. A 15% reduction of friction area by increasing the hull clearance from h = 3.2 m = 10.5 ft to 12.5 ft seems to be possible in smooth water.

From quite a number of towing tests with the Supramar PT 150 model, a simple relationship between the change of hull clearance h (mean value on both foils) and the change of drag ΔD resulted:

$$\frac{\Delta D}{D\ (W.L.2)} = 0.5\,\frac{\Delta h}{h\ (W.L.2)} = \frac{\Delta A_d}{\Sigma A_d\ (W.L.2)} \quad \ldots(14)$$

This relationship has been confirmed by trials of the full scale vessel. Furthermore the relative drag change coincides with the relative change of friction area $\Delta A_d/\Sigma A_d$, all related to the high speed waterline W.L.2. Thus it seems to be justified to rely primarily on the friction area and to neglect the displacement if maximum speed is required.

In fact, many trials of Supramar hydrofoils proved that they are rather insensitive to change of displacement in the foilborne mode. However, it must be kept in mind that the displacement has a marked influence on the drag hump, which in general occurs at a speed $<V_1$ with a partially wetted hull. At this critical condition in a seaway the hydrofoil craft needs a certain thrust margin by which in turn the attainable maximum speed will be limited.

While the maximum speed depends mainly on drag, the take-off speed depends on lift coefficient. Equation (11)

$$C_L = 0.4 + \frac{1}{4}\exp\left(-\frac{c_m}{d_m}\right) = \frac{\Delta}{q\ \Sigma A_p},\quad q = \frac{\zeta}{2}V^2$$

refers to the sum of both foils where the mean area/lift ratio $\Sigma A_p/\Delta$, $\Delta = L_f + L_r$, is plotted as abscissa in Fig 3. Solving the equation for dynamic pressure q yields the following expression for the speed in W.L.1:

$$V_1\ [kt] = \frac{8.5}{\left[C_L\,\frac{\Sigma A_p\ [m^2]}{\Delta\ \ [t]}\right]^{\frac{1}{2}}\ (W.L.1)} \quad \ldots\ldots(15)$$

which was used to determine the induced angle of attack α_i^* equation (6) in W.L.1.

It might be worthwhile to compare the limit of the speed range during foilborne operation V_1 and V_2 equation (13). Similar to the diagrams considered formerly, we use the two speeds as coordinates in Fig 6, where we get again a theoretical boundary, this time $V_2 = V_1$, without any speed range. Nearly all hydrofoil craft are represented by two points, connected by a line, which are designated by m = measured and c = calculated. The maximum speed V_2 of the three US Navy craft is not published but only >40, >45 or >50 — in some cases different figures of V_2 are reported. The take-off speed V_1 is not only sensitive to displacement and longitudinal position of c.g. but also to foil angles of attack and/or flap angle.

Most hydrofoil craft are grouped around the speed ratio $V_2/V_1 = 1.5$ drawn as a straight line together with two other speed ratios. Again — as seen in former diagrams — *Bras d'Or* and *Denison* form, in Fig 6, exceptions, with $(V_2—V_1)/V_1$ which is roughly three times as big as the a speed ratio $V_2/V_1 \approx 2.5$ or a dimensionless speed range average of the remaining hydrofoils. A large speed range is not only advantageous for an ASW-craft like *Bras d'Or* but facilitates the take-off in adverse conditions such as heavy seas, surface roughness, overloading and bow down trim.

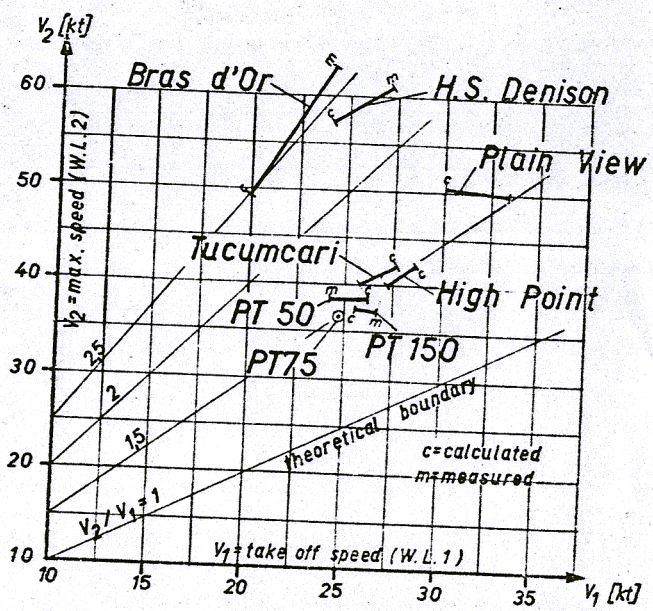

Fig. 6 Speed in Water Line 1 and 2

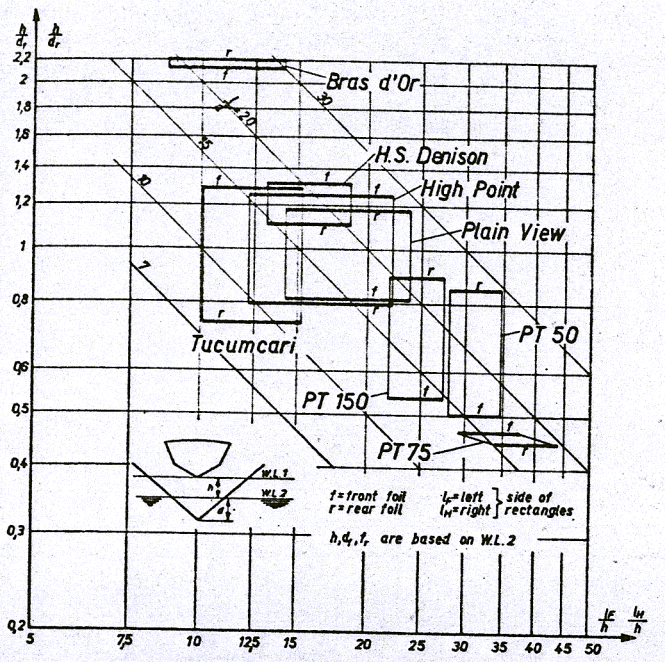

Fig.7 Relations Between Design Hull Clearance h and Foil Submergences d, Ship Length l_H and Foil Distance $l_F < l_H$

The assumed drag increase by 20% during take-off compared with W.L.2 — used in the drag/lift ratio equation (12) — results in the same power requirement in both conditions, providing a speed ratio $V_2/V_1 = 1.2$ and the same overall efficiency. This one in general is decreased for a lower speed but on the other hand the prime mover delivers a higher output during the short period of take-off. With respect to the dimensionless foilborne speed range, Fig 6 shows no clear difference between the Supramar types and the fully submerged American test craft.

Relationship Between Hull Clearance, Foil Submergence, Ship Length and Foil Distance

The behaviour of a hydrofoil ship in a seaway is restricted by certain geometric foil system parameters. Contrary to the aeroplane, which has a large freedom in its height* — relative to its length — the hydrofoil is in danger of leaving its elements. The foil depth of submergence d and the hull clearance h in the high speed waterline reach only some percentage of the craft of which two characteristic lengths l have been chosen and represented in Fig 7, as ratio l/h at the abscissa.

The ordinate of Fig 7 represents the ratio between hull clearance h and foil depth d, that means the lowest point of the foil below the high speed waterline W.L.2, but not necessarily that of the whole foil system. The product of both axes yields the ratio l/d which in the double logarithmic net of Fig 7 is constant on diagonals, of which five are drawn. A good seakeeping capability can be achieved, for a given ship size, with a high hull clearance. In this respect good hydrofoils can be found near the diagonal $l/d = 10$ of Fig 7.

If the vessel is pitching around W.L.2 of one foil, the depth of the other foil limits the maximum pitch angle in one direction and the hull in the other direction. Occurrence of foil broaching is known to the author from the front foils of PT 50 and *Denison*, in heavy seas, and is also reported from other craft. The immersion of the foil after broaching will be less dangerous, if it has some dihedral, as in the cases mentioned.

Hydrofoil craft are especially under strain at the bow, similar to displacement ships, since the largest amplitudes relative to the wave contour occurs at the bow. This experience was confirmed for uncontrolled tandems of a large number of foil parameters, Froude-numbers, wave length and directions, by previous calculations made by the author Ref 15. This result will probably also be valid for controlled fully submerged hydrofoil systems. In a good hydrofoil design we can therefore expect that the depth of submergence d_f at the front foil is larger than d_r at the rear foil. This relationship is represented in Fig 7 by thick lines f below r since the depth of submergence stays in the denominator of the ordinate h/d.

The hydrofoil craft in Fig 7 are represented by rectangles, with the exception of PT 75 due to her different hull clearance at front and rear foil, whose left side refers to the foil distance l_F and whose right side to the length of the hull water line l_H. Considering the left point of the front foils, *Plain View*, PT 150, *Tucumcari* and PT 75, in this series, are in the best position and *Bras d'Or* in the worst one as compared with the diagonals with constant l/d. The right front foil points reveal PT 150, PT 50 and PT 75 as the best craft. Dictated by structural requirements, weight, etc, the largest foil is nearly always provided with the greatest depth of immersion. From this rule Fig 7 shows only *Bras d'Or* and *Denison* as exceptions.* It can be concluded that in respect to the kinematic seaway conditions the aeroplane type foil system offers most advantages.

The design requirements of Fig 7 can be met only partially in heavy seas. More realistic assumptions are made in Fig 8:

(a) mean waterline in the middle of low and high speed waterlines 1 and 2,
(b) half of the design hull clearance h,
(c) foil submergences increased by h/2.

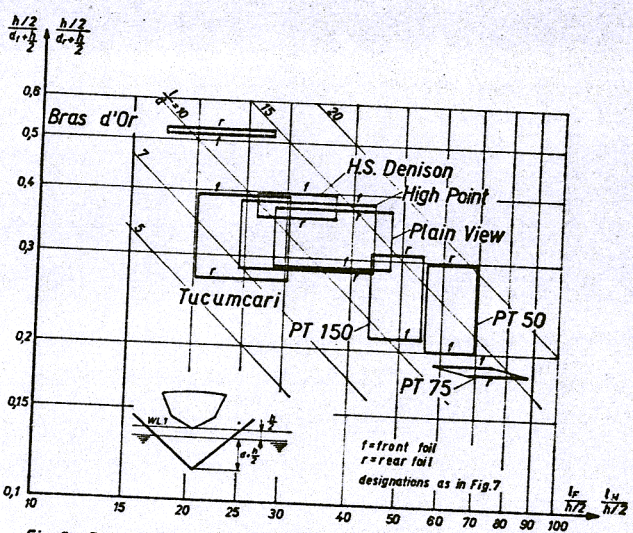

Fig.8 Relations Between Hull Clearance $\frac{h}{2}$ and Foil Submergences $(d+\frac{h}{2})$ in a Sea way, Ship length l_H and Foil Distance $l_F < l_H$

* Except during take-off and landing.

* The PT 75 seems to be a third exception since $h_f/d_f > h_r/d_r$. But these ratios are consistent with the already mentioned hull clearances $h_f = 0.7$ m, $h_r = 0.6$ m and the normal relationship between the depths of submergence $d_f = 1.5$ m, $d_r = 1.355$ m.

The relationship between the rectangles in Fig 8 resembles very much those of Fig 7 but their position in relation to the diagonals is different. Looking for the left point of front foils, we get the following range: *Tucumcari, Plain View, Bras d'Or* and PT 150 as the best craft and PT 50 as the worst one. On the other hand, *High Point* is the worst craft with respect to the right point of the front foil in Fig 8 (length of hull waterline l_H) and PT 150 the best one. As average it can be stated that with regard to the danger of foil broaching in a seaway neither the fully submerged nor the surface piercing front foil is preferred.

Summary

Three Supramar hydrofoil types and five American test craft have been investigated with relation to geometric and hydrodynamic parameters. The main purpose was to compare the surface piercing with the fully submerged system.

Since the foil system is independent of the system of power transmission, the two main foil systems can be compared after elimination of oblique shaft, Z-drive or water jet. The lowest *ratio between frictional and lifting area* (a) in the high speed waterline can be realised by the surface piercing system (best value $a = 1.134$ at front foil of Supramar type PT 50). Fully submerged foil systems as well as the average of all fully submerged tandems are connected with relatively higher frictional area than the corresponding surface piercing ones. This statement also remains valid for the low speed waterline (take-off condition).

Considering the *power transmission* with respect to the drag increase caused by it we find that in the high speed waterline the inclined shaft arrangement permits about 6% lower drag as a percentage of the total drag than the Z-drive. This relationship is inverted during take-off. The water jet needs a rather large water intake whose additional drag seems to be in the whole foilborne range as high as the worst figures mentioned for propeller propulsion (20% of total drag).

A high *foil loading* up to nearly 8 t/m² is possible for surface piercing and fully submerged foils. On the other hand, loadings below 3 t/m² are realised by both foil types. In the high speed water line the average loading amounts to 6.0 – 6.5 t/m² independent on the foil system. In the low speed waterline (take-off condition) the average loading of Supramar surface piercing foils decreases to about 4.4 t/m².

Since the main drag of a hydrofoil is frictional drag, the maximum speed can be approximated by the available power and the submerged friction area. Supplementing the known power/displacement ratio by the friction area/displacement ratio the last one on average shows no difference between fully submerged and surface piercing systems. Correspondingly the two foil systems without power transmission reveal nearly the same *drag/lift ratio* in the high speed waterline. A similar result can be deduced for take-off speed.

A clear advantage of the considered fully submerged foils over surface piercing ones in respect to seaworthiness is their relatively deep *submergence*. This advantage must be paid for by additional complications of the foil retraction mechanism.* The rigid Supramar foils considered have roughly the same mean submergence depth as mean chord length. This ratio depends only little on the position of the waterline, contrary to fully submerged foils. The relative submergence depth ratios of *Bras d'Or* and *Denison* are the lowest ones of the eight hydrofoil systems investigated.

A deep submergence, compared with chord length, is not only advantageous for seakeeping capability but also during take-off. The maximum allowable lift coefficient of straight fully submerged foils is higher than that of surface piercing hydrofoils. The lower take-off lift coefficient of the last group is more than compensated by their smaller foil loading resulting in a lower *take-off speed*. The foil system seems to have no marked influence on the ratio between the maximum and take-off speed, which can be taken 3/2 as average. Only the two aforementioned craft reach a higher ratio of about 5/2.

The *induced angle* is part of the drag/lift ratio. Treating the tandem as a single foil, two groups of hydrofoil craft in relation to the three-dimensional effect can be discriminated:

(a) split foil systems with a small induced angle,
(b) non-split systems with considerably larger induced angle.

However, the low value of the first group probably will be increased by deviations from the ideal lift distribution along the span. On the other hand, the wave making drag of the non-split Supramar system is decreased by favourable interference between both foils. The least wave drag can be expected for the fully submerged systems.

* In the event that the vessel has also to be used in shallow harbours.

References

1. E. K. Sullivan, J. A. Higgins: Tests and Trials of the H.S. *Denison*.
2. G. J. Wennagel: Characteristics of the US Maritime Administration Hydrofoil Test Craft. US Dep of Commerce, Maritime Administration, Washington 25 DC.
3. J. C. Schroeder: The Design, Construction and Flight Test of the HS *Denison*. Proceedings of the National Meeting on "Hydrofoil and/or Cushion Vehicles". September 17–18, 1962.
4. W. M. Ellsworth: The US Navy Hydrofoil Development Program — a Status Report. AIAA/SNAME Advance Marine Vehicles Meeting Norfolk, Virginia, May 22–24, 1967.
5. D. M. Petrie: High Point. 1965.
6. M. C. Eames, E. A. Jones: HMCS *Bras d'Or* — An Open Ocean Ship. Meeting of The Royal Institution of Naval Architects, London, on April 22, 1970.
7. Jane's Surface Skimmer Systems 1968–69. Samson Low, Marston Co Ltd, London.
8. S. F. Hoerner: Fluid Dynamic Drag. Published by the Author, 1958.
9. E. Truckenbrodt: Die Berechnung des Profilwiderstandes aus der vorgegebenen Profilform. Ing. Archiv 21, 1953.
10. Schlichting/Truckenbrodt: Aerodynamik des Flugzeuges. Springer-Verlag Berlin 1960.
11. I. H. Abbot, A. E. von Doenhoff: Theory of Wing Sections. Dover publications, Inc, New York, 1959.
12. E. Faber: Hydrofoil Craft and Their Marine Engineering Aspects. The Institute of Marine Engineers, London, March 24, 1970.
13. G. Gabrielli, Th. von Karman: What Price Speed? Mechanical Engineering, 1950, pp 775–781.
14. H. de Witt: Hydrodynamic Study on Fully Submerged Foils of Hydrofoil Ships in a Seaway up to 140 kt at Constant Froude Number. *Hovering Craft and Hydrofoil*, February 1969, p 24–43.
15. H. de Witt: Lineare Theorie der symmetrischen Schwingungen von Tragflügeltandems in flachen, sinusförmigen Wellen. Dissertation Braunschweig 1966. Available by the author, c/o Supramar AG, Lucerne.